EurJIC
European Journal of Inorganic Chemistry

Full Papers
doi.org/10.1002/ejic.202100485

Chemistry Europe
European Chemical Societies Publishing

Mitochondrial Targeting Cationic Purpurinimide–Polyoxometalate Supramolecular Complexes for Enhanced Photodynamic Therapy with Reduced Dark Toxicity

Tae Heon Lee,[a] Yang Liu,[a] Hye Jeong Kim,[a] Sang Hyeob Lee,[a] Hyeon Ho Song,[a] Young Key Shim,[a] Woo Kyoung Lee,*[a] and Il Yoon*[a]

Polyoxometalates (POMs), that are well-defined metal-oxygen cluster anions, are functional molecules extensively used in various research applications. The synthesis of neutral purpurinimides, followed by conversion to cationic purpurinimides (CPIs), formed CPI–POM supramolecular complexes via electrostatic interactions between each CPI and the polyanionic POM. The cellular uptake of purpurinimides, CPIs, and their CPI–POMs in A549 and HeLa cell lines was confirmed by confocal laser scanning microscopy. CPIs showed concentration-dependent dark cytotoxicity; however, CPI–POMs exhibited reduced low dark cytotoxicity. After photoirradiation, CPIs and CPI–POMs revealed enhanced photodynamic therapy (PDT) compared to free purpurinimides against A549 and HeLa cells. The CPIs exhibit low cell viability by incorporating their PDT effect with intrinsic dark cytotoxicity; however, the CPI–POMs exhibited a POM delivery effect-based enhanced PDT activity in the supramolecular complex system with low dark cytotoxicity. In particular, the clicked CPI–POM revealed two times higher PDT activity compared with the clicked free CPI, due to the good delivery effect of POM.

Introduction

Cationic chlorins and porphyrins are expected to exhibit increased cellular penetration and retention in tumour cells, making them useful for applications such as DNA binding/photocleavage[1–4] and for use as photosensitizers (PSs) for photodynamic therapy (PDT).[5–8] A type of click chemistry reaction, copper (I)-catalysed alkyne-azide cycloaddition, has attracted much attention because of its straightforwardness, mild conditions, and high yields, allowing for the synthesis of functionally modified and conjugated molecules that have wide applications.[9–12] PDT is a promising non-invasive and patient-specific cancer treatment with minimal side effects, which is based on the administration and selective accumulation of a PS in tumour tissue, to generate cytotoxic reactive oxygen species (ROS), especially singlet oxygen ($^1O_2$), after photoirradiation. These cytotoxic species inflict direct cellular damage, destroy tumour vascularization, and trigger subsequent inflammatory and immune cell destruction.[13–23] However, the clinical application of PDT is hampered by the need to increase cellular penetration without causing aggregation, light penetration with long wavelength absorption, and prevention of dark toxicity of PSs for enhanced PDT activity with few side effects.[15,24–30]

Recently, we have developed delivery systems for better cellular uptake of PSs into tumour cells using gold nanoparticles (sphere and rod types)[31–35] and polyoxometalate (POM) complexes.[36] POMs, which are metal-oxygen cluster anions, are functional molecules extensively used in various applications owing to their favourable catalytic, photochemical, and electrical properties.[37–39] Importantly, there are very rare biomaterial applications of POM-based supramolecular materials those built on electrostatic interactions.[40–44] In a previous report,[36] we demonstrated a chlorin–POM supramolecular complex that showed enhanced photodynamic activity compared to free chlorin. This POM complex exhibited excellent PS delivery, owing to the stable and strong electrostatic interactions between polyanionic POM and cationic chlorins. Among the chlorins, purpurinimides have attracted attention because of their unique advantages, such as long wavelength absorption to permit deeper light penetration at tumour sites, high extinction coefficient at an appropriate wavelength, good $^1O_2$ photogeneration, and low hydrophobicity.[5,19,22,45–48] In the supramolecular system, POM plays an important role as a delivery vehicle (polar attractor) of cationic purpurinimides (CPIs) into tumour cells via endocytosis (Figure 1).[49]

However, the disadvantages of the reported chlorin–POM complex are its short wavelength absorption (maximum absorption wavelength [λ_{max}] 665 nm in CH_2Cl_2), that prevents deep tissue penetration, as well as high IC_{50} value (6.61 μM at 48 h and 8.60 μM at 24 h incubation times) due to the very low photodynamic activity of the free cationic chlorin ($IC_{50} > 20$ μM) in the tumour cells.[36] To overcome these limitations, we herein report the design and synthesis of new CPIs and the preparation of their POM complexes (CPI–POMs), that show long wavelength absorption (λ_{max} 707 nm in CH_2Cl_2), and therefore permit deeper light penetration at tumour sites and

[a] T. H. Lee, Dr. Y. Liu, H. J. Kim, S. H. Lee, H. H. Song, Prof. Dr. Y. K. Shim, Prof. Dr. W. K. Lee, Prof. Dr. I. Yoon
Center for Nano Manufacturing and Department of Nanoscience and Engineering
Inje University
197 Injero, Gimhae, Gyeongnam 50834, Republic of Korea
E-mail: yoonil71@inje.ac.kr
wlee@inje.ac.kr

Supporting information for this article is available on the WWW under https://doi.org/10.1002/ejic.202100485

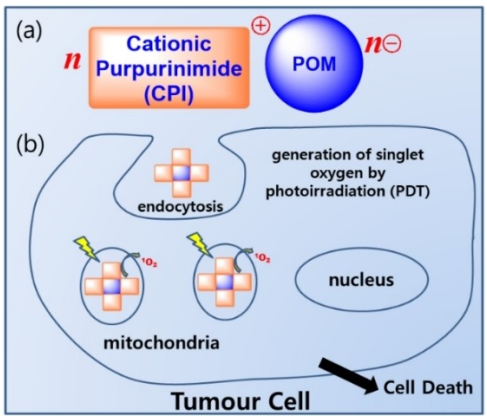

Figure 1. (a) Formation of a CPI–POM supramolecular complex via electrostatic interactions. (b) Proposed mechanism for the cellular uptake followed by mitochondrial targeting of CPI–POM complexes into tumour cells through endocytosis, causing cell death after photogeneration of $^1O_2$, resulting in enhanced photodynamic activity.

high photodynamic activity. Purpurinimides, CPIs, and CPI–POMs accumulated in A549 and HeLa cells, and exhibited mitochondrial targeting, inducing mitochondria-mediated apoptosis to destroy the tumour cells.[50–54] The CPIs and CPI–POM complexes exhibited significantly enhanced (highly decreased) IC_{50} values compared to the corresponding free neutral purpurinimides. More importantly, while the CPIs showed concentration-dependent dark toxicity, CPI–POM complexes showed highly reduced dark toxicity. These findings indicate that CPI–POM complexes are potential PS candidates for enhanced PDT with reduced dark toxicity.

Results and Discussion

Characterisation of Purpurinimides and their CPIs and CPI–POM complexes

The synthesis of purpurinimides and their cationic forms is straightforward (Scheme 1a). Extraction of chlorophyll-a paste with acidic methanol (5% H_2SO_4 in MeOH) afforded methylpheophorbide a (MPa) as an important starting material.[55] MPa was further converted to purpurin-18 methyl ester (P18ME) under basic conditions, affording the purpurinimide derivatives **1** and **2** after reaction with the corresponding amine, *N,N*-dimethylbutylamine and 4-picolylamine, respectively. *N*-Propargyl purpurinimide methyl ester (NPPME) was obtained from the reaction of P18ME with propargyl amine, and then used in a click reaction utilising copper iodide (CuI, 10 mol%) and diisopropylethylamine (DIPEA) in CH_2Cl_2, which furnished a triazole ring to generate clicked purpurinimide **3**. Methylation of each purpurinimide derivative **1**–**3** with methyl iodide (MeI) afforded the corresponding CPI derivatives **1**+–**3**+, as dark green solids in quantitative yield without further purification.

All reaction steps were monitored by TLC and UV-Vis absorption spectroscopy. In addition, all the compounds were fully characterised by ^{1}H-NMR, UV-Vis spectroscopy, and HRFABMS.

To introduce POM, we used the well-known Keggin-type POM **4**,[36,56] $[\alpha\text{-}SiMo_{12}O_{40}]^{4-}$, which was prepared according to a procedure previously described in literature, and was soluble in common organic solvents such as acetonitrile in its organic salt form (e.g. tetrabutylammonium). Combining POM and four equivalents of each CPI (**1**+, **2**+, and **3**+) in acetonitrile afforded the CPI–POM complexes (**1**+**POM**, **2**+**POM**, and **3**+**POM**) as dark green solids (precipitates) in good yield (70%–73%, Scheme 1b), exhibiting the stable and strong electrostatic interactions between polyanionic POM and CPIs.

The structures of all compounds were characterised by ^{1}H-NMR, UV-Vis, and FTIR spectroscopy, and HRFABMS (Supporting Information, Figures S1–S17). The ^{1}H-NMR spectrum of NPPME shows one triplet signal at 2.31 ppm ($J = 2.4$ Hz) and multiplet signals at 5.35–5.32 and 5.31–5.23 ppm in $CDCl_3$, corresponding to characteristic alkyne (C≡CH) and N-CH_2 protons, respectively (Figure S3).[57] The ^{1}H-NMR spectra of neutral purpurinimide derivatives **1**, **2**, and **3**, their cationic forms **1**+, **2**+, and **3**+, and their complexes **1**+**POM**, **2**+**POM**, and **3**+**POM** are shown in Figure 2, Figure 3, and Figure 4, respectively. All proton signals were fully assigned, and each signal of the *N*-alkyl group attached to the six-membered imide ring is highlighted in blue. Furthermore, the chemical shift changes are shown as dashed lines. The proton signal of N^5 in **1**+ was significantly downfield-shifted (~0.8 ppm) from **1**. All proton signals on benzyl pyridine in **2**+ were shifted downfield compared with the neutral form **2**. In particular, N^2 and N^3 signals on the pyridine unit in **2**+ were highly downfield shifted. The ^{1}H-NMR spectrum of **3** featured a key triazole signal (N^2, singlet) at 8.48 ppm, indicating a successful click reaction, as well as signals of the pyridine unit at 8.66 and 7.76 ppm. The ^{1}H-NMR spectrum of clicked CPI **3**+ displays the pyridinium salt signal at 4.11 ppm (broad singlet), indicating successful methylation, as well as two broad singlets of the pyridine unit at 8.74 and 8.31 ppm. No signals of the tetrabutylammonium cation (present in the starting POM **4**, Figure S5) were detected for any of the POM complexes, indicating complete cation exchange with each CPI, which leads to a 4:1 CPI:POM ratio (Scheme 1b).

HRFABMS analysis confirmed the formation of **1** (calcd. for $[M+H]^+$ 677.3815; found 677.3818) (Figure S8), **1**+ (calcd. for $[M]^+$ 691.3966; found 691.3977) (Figure S9), **2** (calcd. for $[M+H]^+$ 669.3189; found 669.3192) (Figure S10), **2**+ (calcd. for $[M]^+$ 683.3340; found 683.3342) (Figure S11), **3** (calcd. for $[M+H]^+$ 736.3360; found 736.3357) (Figure S12), and **3**+ (calcd. for $[M]^+$ 750.3511; found 750.3513) (Figure S13). The FTIR spectrum of **4** displayed signals specific to POM, such as Si=O, Mo=O, and Mo–O–Mo stretches at 951 cm^{-1}, 899 cm^{-1}, and 804 cm^{-1}, respectively (Figure S6). The absorption spectra of all purpurinimides, their CPIs, and their CPI–POM complexes, were recorded in DMSO (Figure 5). The maximum absorption wavelengths (λ_{max}) were progressively red-shifted for MPa (668 nm), P18ME (700 nm), NPPME (707 nm), and **1**–**3** (707 nm) (Figure 5, Figure S2, and Figure S4). In purpurinimide derivatives with various alkyl groups, the λ_{max} values of the purpurinimide core remained unchanged, even in both cationic and POM complex

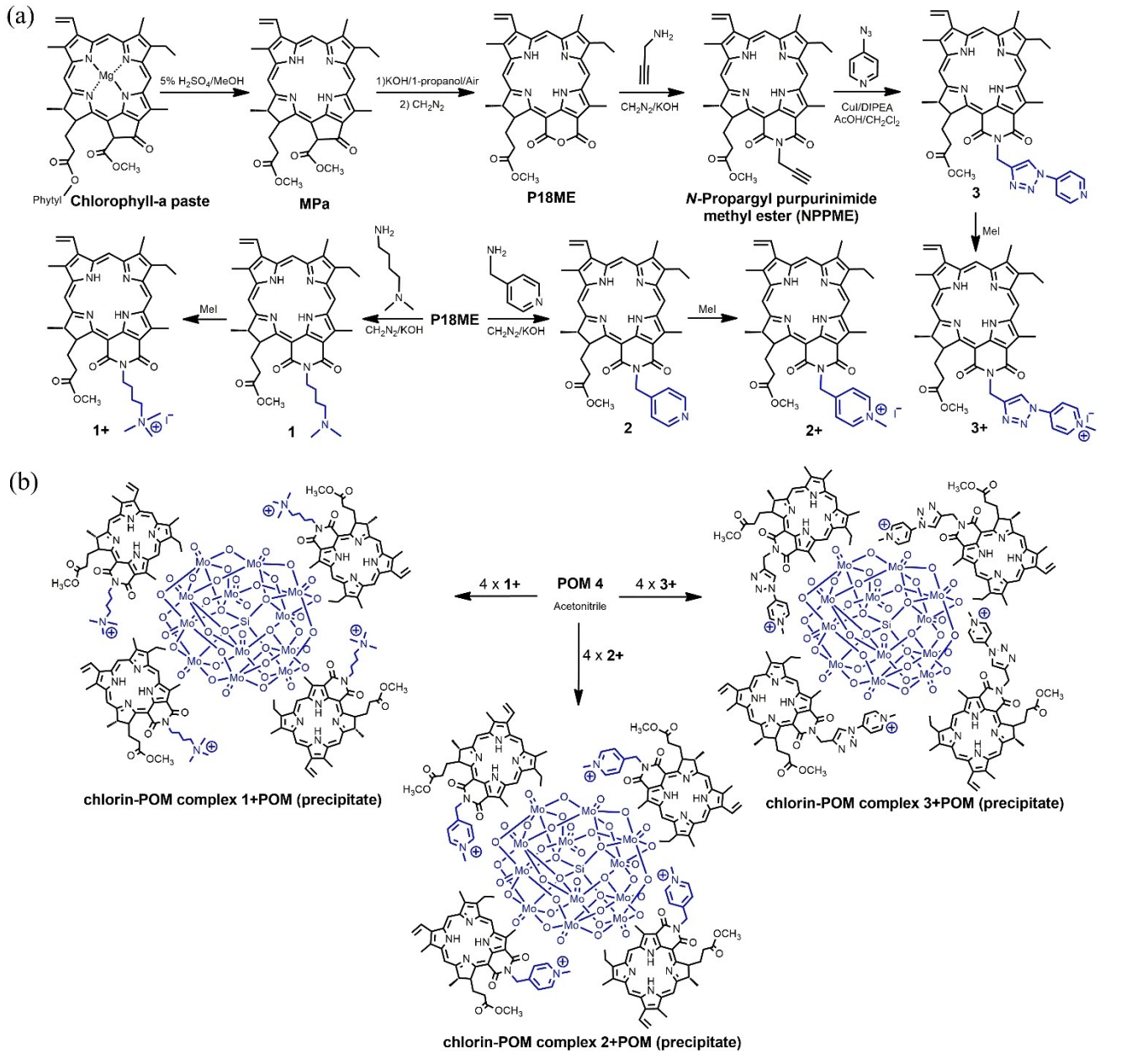

Scheme 1. (a) Synthesis of purpurinimide derivatives **1**–**3** and their CPI forms (ammonium, pyridinium, and clicked pyridinium) **1+**, **2+**, and **3+**. (b) Synthesis of CPI–POM complexes **1+POM**, **2+POM**, and **3+POM.**

forms. In addition, TGA analysis (Figures S14–S16) of **1+POM**, **2+POM**, and **3+POM** showed 60–62 wt% of organic content (four CPI units) and 40–38 wt% of inorganic content (one POM unit), confirming a 4:1 ratio (CPI:POM), as shown in Scheme 1.

Cellular Uptake and Localization

The cellular penetration and localisation of purpurinimides, CPIs, and CPI–POM complexes in A549 and HeLa cells before *in vitro* irradiation were confirmed by confocal laser scanning microscopy (CLSM, Figure 6, Figure 7).[58,59] Fluorescence of the purpurinimide or CPI molecules (red colour) of all compounds was detected inside the cells, indicating successful cellular uptake of purpurinimide or CPI in the cytoplasm of the tumour cells. In particular, all the purpurinimide or CPI molecules showed mitochondrial targeting (orange colour in merged images) inducing mitochondria-mediated apoptosis to destroy the tumour cells after photoirradiation.[50–54]

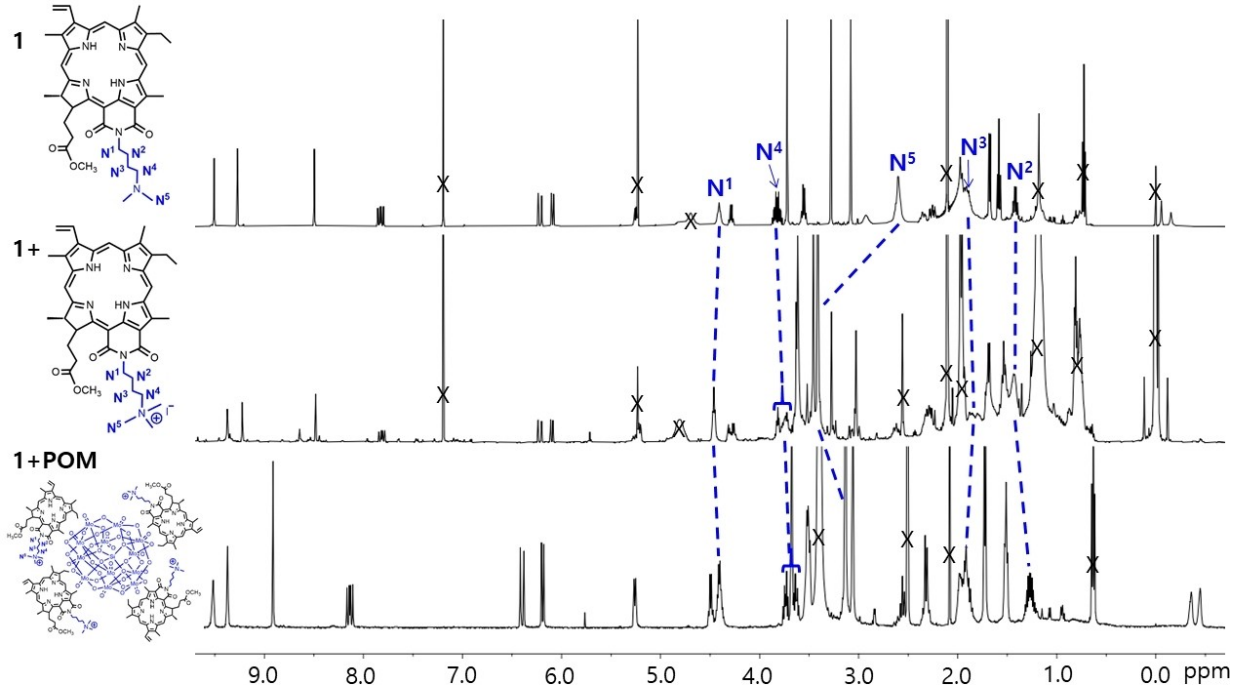

Figure 2. ^{1}H-NMR spectra of purpurinimide **1** and CPI **1+** in $CDCl_3$, and **1+POM** complex in DMSO-d_6 (500 MHz, 298 K).

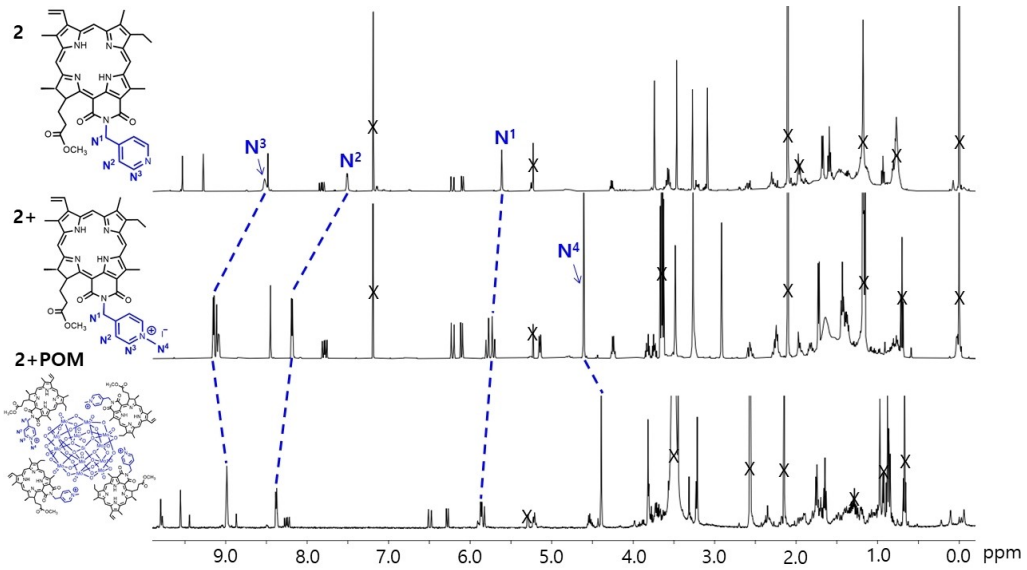

Figure 3. ^{1}H-NMR spectra of purpurinimide **2** and CPI **2+** in $CDCl_3$, and **2+POM** complex in DMSO-d_6 (500 MHz, 298 K).

Morphological Changes with Photoirradiation

After irradiation with a halogen lamp equipped with a band-pass filter (640–710 nm) (total light dose 2 J cm^{-2}, irradiation time 15 min), the cells treated with **3+** (Figure 8b) and **3+POM** (Figure 8c) exhibited morphologies different from those treated with **3** (Figure 8a), due to the formation of apoptotic bodies, owing to the higher photodynamic activity of the former compared to **3** at a concentration of 1 μM.[39,60] This result was confirmed using fluorescence microscopy of live (green)/dead (red) cells stained with calcein AM/PI. Compound **3+** (Figure 8e) and complex **3+POM** (Figure 8f) killed more cells than compound **3** (Figure 8d), which was in agreement with the morphological changes shown in Figures 8a–c.

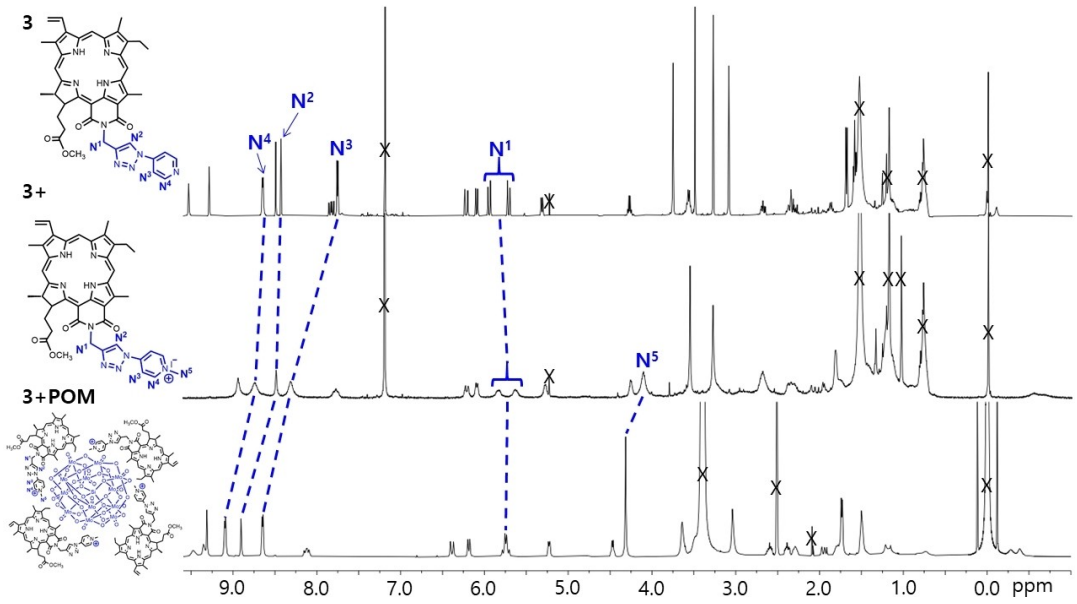

Figure 4. ^{1}H-NMR spectra of purpurinimide **3** and CPI **3+** in $CDCl_3$, and **3+POM** complex in DMSO-d_6 (500 MHz, 298 K).

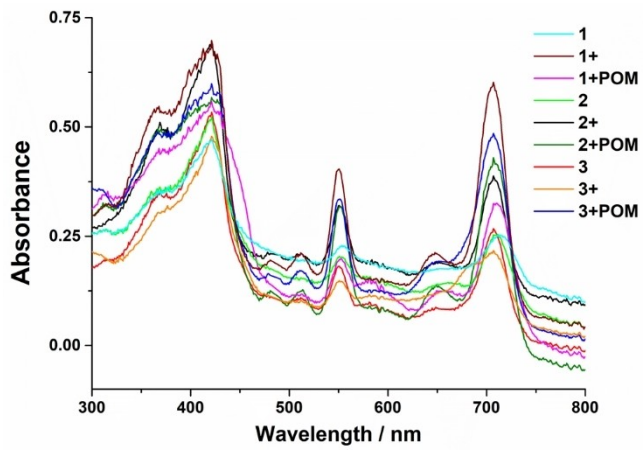

Figure 5. UV-Vis absorption spectra (10 μM in DMSO at 25 °C) of free PSs, cationic PSs, and their POM complexes.

Cell Viabilities for Photocytotoxicity and Dark Cytotoxicity

Photo- and dark cytotoxicities of **1**–**3**, **1+**–**3+**, and **1+POM**–**3+POM** were investigated at a concentration range of 0.25–20 μM, and incubation periods of 3 h and 24 h, against A549 and HeLa cells (Figure 9). Each cell (10×10^4 cells/well) was incubated with PSs for 24 h, and photoirradiated for the photocytotoxicity test (total light dose 2 J cm^{-2}, irradiation time 15 min). After photoirradiation of cells incubated for 3 h and 24 h, their viability (%) was estimated based on the mitochondrial activity of NADH (reduced form of nicotinamide adenine dinucleotide) dehydrogenase using the MTT cell viability assay (summarised in Tables S1–S4).

Dark toxicity was different for different cell types (A549 and HeLa). In A549 cells, all cationic PSs **1+**–**3+** showed concentration-dependent dark cytotoxicity, owing to the characteristic properties of these cationic PSs.[61,62] Also, **3** (neutral form) showed concentration-dependent dark cytotoxicity than others. However, none of the POM complexes, **1+POM**–**3+POM**, showed dark cytotoxicity, which indicates that POM complexes are potential PS candidates. This result is consistent with that of our previous study.[36] On the other hand, in HeLa cells, all neutral and cationic PSs showed concentration-dependent dark cytotoxicity. However, POM complexes displayed highly reduced dark cytotoxicity, possibly because of the electrostatic interactions between the cationic purpurinimides and anionic POMs, which mitigated the toxicity of free CPI. **1+POM** and **2+POM** showed concentration-dependent dark toxicity after 3 h incubation, but negligible dark toxicity after 24 h incubation. Notably, **3+POM** showed no dark toxicity.

Upon photoirradiation, the cell viability decreased for all compounds, a finding consistent with the observation of increased concentration and incubation time. Furthermore, cell viability was dependent on the cell type. In A549 cells, each cationic form showed better results than the corresponding free purpurinimides, which might be because of the electrostatic interaction between the CPI and the cell, followed by accumulation in the cells. Even though the cationic form, **1+** and **2+**, showed almost identical therapeutic activities (0.14 μM and 0.18 μM of IC_{50} after 3 h of incubation; 0.13 μM and 0.15 μM of IC_{50} after 24 h of incubation, respectively) (Table 1) compared with the POM complex, **1+POM** and **2+POM**, (0.14 μM and 0.14 μM of IC_{50} after 3 h of incubation; 0.13 μM and 0.13 μM of IC_{50} after 24 h of incubation, respectively) the high photoactivity led to concentration-dependent dark toxicity. However, the POM complexes showed no dark toxicity, indicating that the high photoactivity of the POM complexes is a sign of good delivery effect of the POM in the POM complexes. Furthermore, **3+POM** (0.37 μM and 0.17 μM

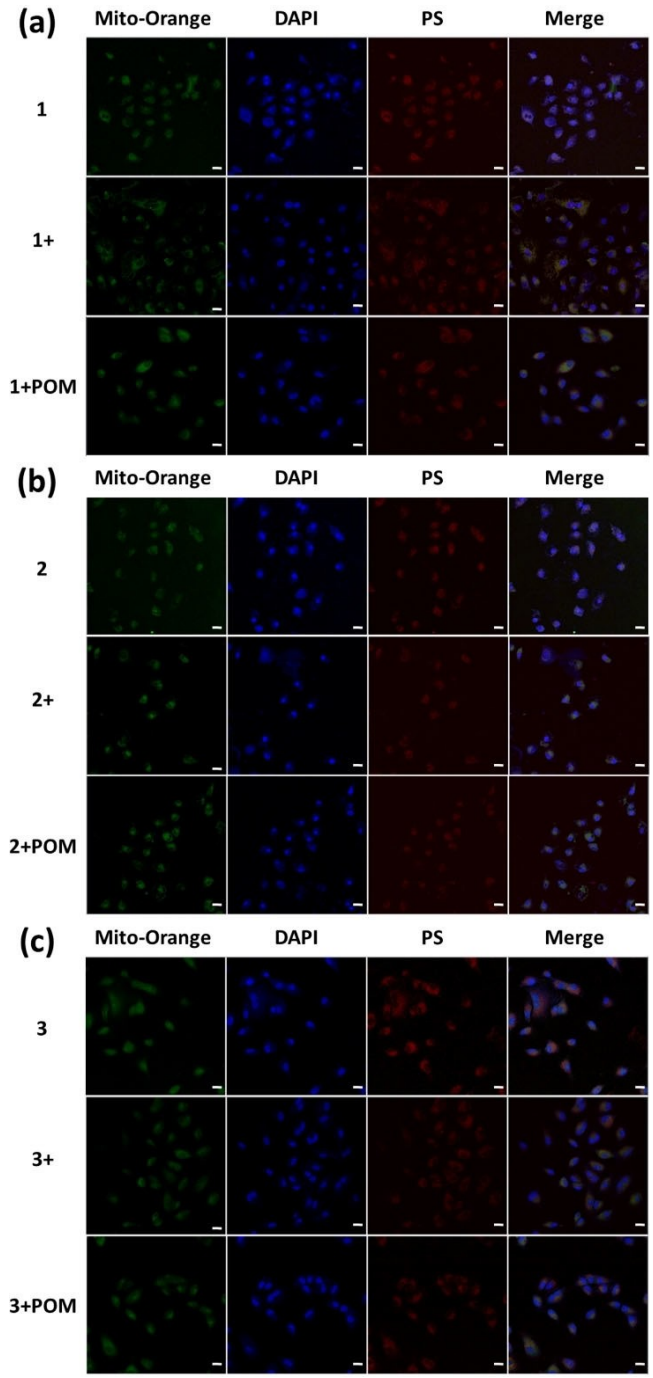

Figure 6. Cellular uptake using CLSM images of A549 cells before irradiation at 6 h post-incubation for (a) **1**, **1+**, **1+POM**, (b) **2**, **2+**, **2+POM**, (c) **3**, **3+**, **3+POM** (the concentration of PS is 1 μM in each sample): DAPI nuclear dye (blue), PS (red), Mito-Orange mitochondrial dye (green) and merged images. Scale bar: 20 μm.

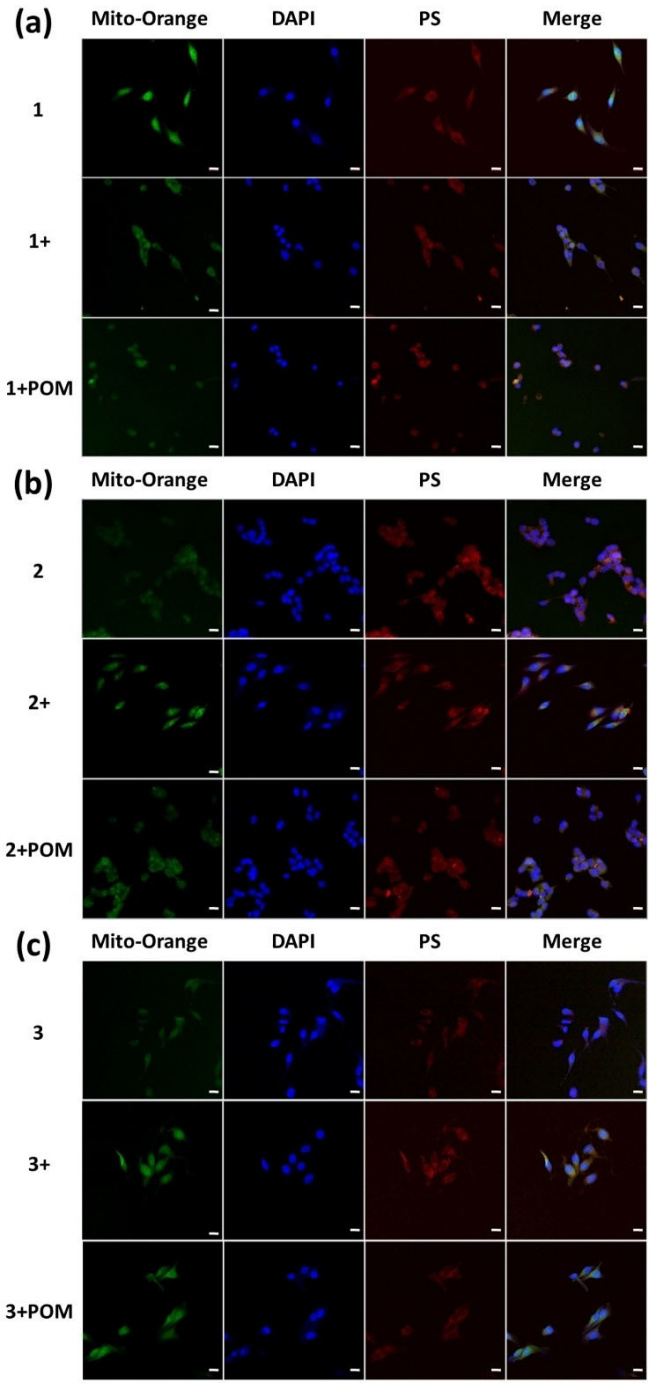

Figure 7. Cellular uptake using CLSM images of HeLa cells before irradiation at 6 h post-incubation for (a) **1**, **1+**, **1+POM**, (b) **2**, **2+**, **2+POM**, (c) **3**, **3+**, **3+POM** (the concentration of PS is 1 μM in each sample): DAPI nuclear dye (blue), PS (red), Mito-Orange mitochondrial dye (green) and merged images. Scale bar: 20 μm.

of IC_{50} after 3 h and 24 h of incubation, respectively) displays two times higher photoactivity when compared with its cationic form **3+** (0.69 μM and 0.48 μM of IC_{50} after 3 h and 24 h of incubation, respectively) indicating good delivery effect of the POM complex. Interestingly, the photoactivities (IC_{50}) of **1+** and **1+POM** after 3 h of incubation were the same as those after 24 h of incubation, which could indicate a very fast intracellular uptake of **1+**, possibly because of the high flexibility of the *N*-alkyl group. This phenomenon is consistent with the results of our previous study.[45] In HeLa cells, each CPI and its POM complex showed identical photoactivities after 24 h of incubation. In both A549 and HeLa cells, **1+** and **1+POM**, and **2+**

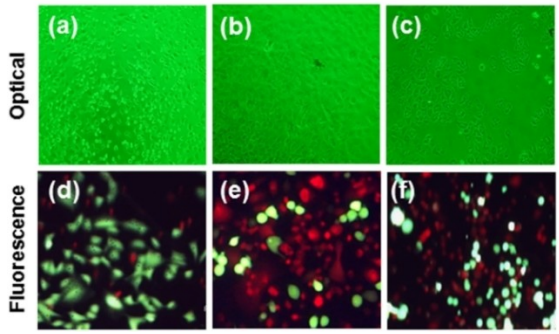

Figure 8. Optical images of A549 cells after treatment with **3** (a), **3+** (b), and **3+POM** (c); fluorescence images of live (green)/dead (red) cells stained with calcein AM/PI after 3 h of incubation with **3** (d), **3+** (e), and **3+POM** (f) and photoirradiation. The concentration of each PS was 1 μM.

and **2+POM** showed almost identical photoactivities after 24 h of incubation (IC_{50}: 0.13 μM and 0.13 μM, and 0.15 μM and 0.13 μM in A549; 0.14 μM and 0.14 μM, and 0.14 μM and 0.14 μM in HeLa, respectively). On the other hand, **3+** and **3+POM** showed better photoactivities in HeLa cells after 24 h of incubation, compared with those in A549 cells (IC_{50}: 0.12 μM and 0.12 μM in HeLa; 0.48 μM and 0.17 μM in A549, respectively). POM **4** displayed low phototoxicity, which almost equalled the dark cytotoxicity. It is noteworthy that POM complexes exhibit very high phototoxicity and very low dark cytotoxicity, making them potential PS candidates for PDT. POM complexes display advantageous, stable, and strong electrostatic interactions between POM and the four CPI moieties, playing an important role not only as a delivery vector for CPIs (as polar attractor),[39] but also as a reducer of their dark cytotoxicity.

Singlet Oxygen Photogeneration

Figure 10 highlights the relative differences between $^1O_2$ photogeneration by all the compounds using DPBF as a selective $^1O_2$ acceptor.[63] Compounds **2**, **2+**, and **2+POM** showed $^1O_2$ photogeneration that was almost identical to that of MB (standard $^1O_2$ acceptor).[64,65] Interestingly, **2+POM** and **3+POM** showed slightly lower $^1O_2$ photogeneration than **2** and **2+** and **3** and **3+** in the absence of tumour cells; however, the POM complexes showed better or comparable PDT activity compared with free forms (neutral and cationic PSs), which indicates that the enhanced photodynamic activity of POM complexes based-on the good delivery effect of POM results from the high cellular penetration and localisation of the purpurinimide moieties of POM complexes in tumour cells via endocytosis, as compared to free purpurinimides.[41,66]

Conclusion

In conclusion, we synthesised CPI derivatives, such as ammonium, pyridinium, and clicked pyridinium salt, which were then used to prepare CPI–POM supramolecular complexes, showing long-wavelength absorption (λ_{max} 707 nm) and cellular uptake followed by mitochondrial targeting, inducing mitochondria-mediated apoptosis after photoirradiation to destroy the tumour cells. The CPIs and their CPI–POM complexes exhibited a significantly enhanced PDT effect against A549 and HeLa cells (IC_{50} 0.12–0.48 μM after 24 h of incubation) compared with neutral purpurinimide derivatives. The CPIs and their CPI–POM complexes of ammonium (**1+** and **1+POM**) and pyridinium (**2+** and **2+POM**) exhibited almost identical PDT activities against A549 and HeLa cells, those might be attributed by high photoactivity of each cationic PS itself. Interestingly, the clicked CPI–POM complex (**3+POM**, IC_{50} 0.17 μM) exhibited two times better PDT activity than the free clicked CPI (**3+**, IC_{50} 0.48 μM) after 24 h of incubation against A549 cells, revealing the good delivery effect of POM. Importantly, while the CPIs displayed concentration-dependent dark cytotoxicity, the CPI–POM complexes showed very low dark toxicity, making them potential PS candidates for PDT. Therefore, this CPI–POM supramolecular complex could not only be a useful PS, but could also serve as a suitable delivery vector with reduced side effects in clinical applications. In addition, for further medicinal application using these CPI–POM complexes, we considering that it is need to increase low stability of the CPI–POM complexes in the physiological environment (Table S5 and Figures S17–S18 in the Supporting Information) as a future study.

Experimental Section

Materials

All chemical reagents used in this experiment were of analytical grade and required no further purification, including potassium hydroxide (KOH), sulfuric acid (H_2SO_4), nitric acid (HNO_3), acetic acid (AcOH), anhydrous sodium sulfate, tetrabutylammonium chloride

Table 1. IC_{50} (μM) values of various purpurinimides and their cationic and POM complex forms against A549 and HeLa cells after 3 h and 24 h of incubation after irradiation (total light dose: 2 J/cm^2 with LED for 15 min), respectively.

Cell type	Incubation time	1	1+	1+POM	2	2+	2+POM	3	3+	3+POM
A549	3 h	0.87	0.14	0.14	1.82	0.18	0.14	12.42	0.69	0.37
	24 h	0.46	0.13	0.13	0.93	0.15	0.13	0.94	0.48	0.17
HeLa	3 h	0.34	0.20	0.31	0.31	0.29	0.22	0.48	0.19	0.18
	24 h	0.17	0.14	0.14	0.17 (0.19)[a]	0.14	0.14	0.32	0.12	0.12

[a] Reference [19] by WST-8 assay after 12 h of incubation.

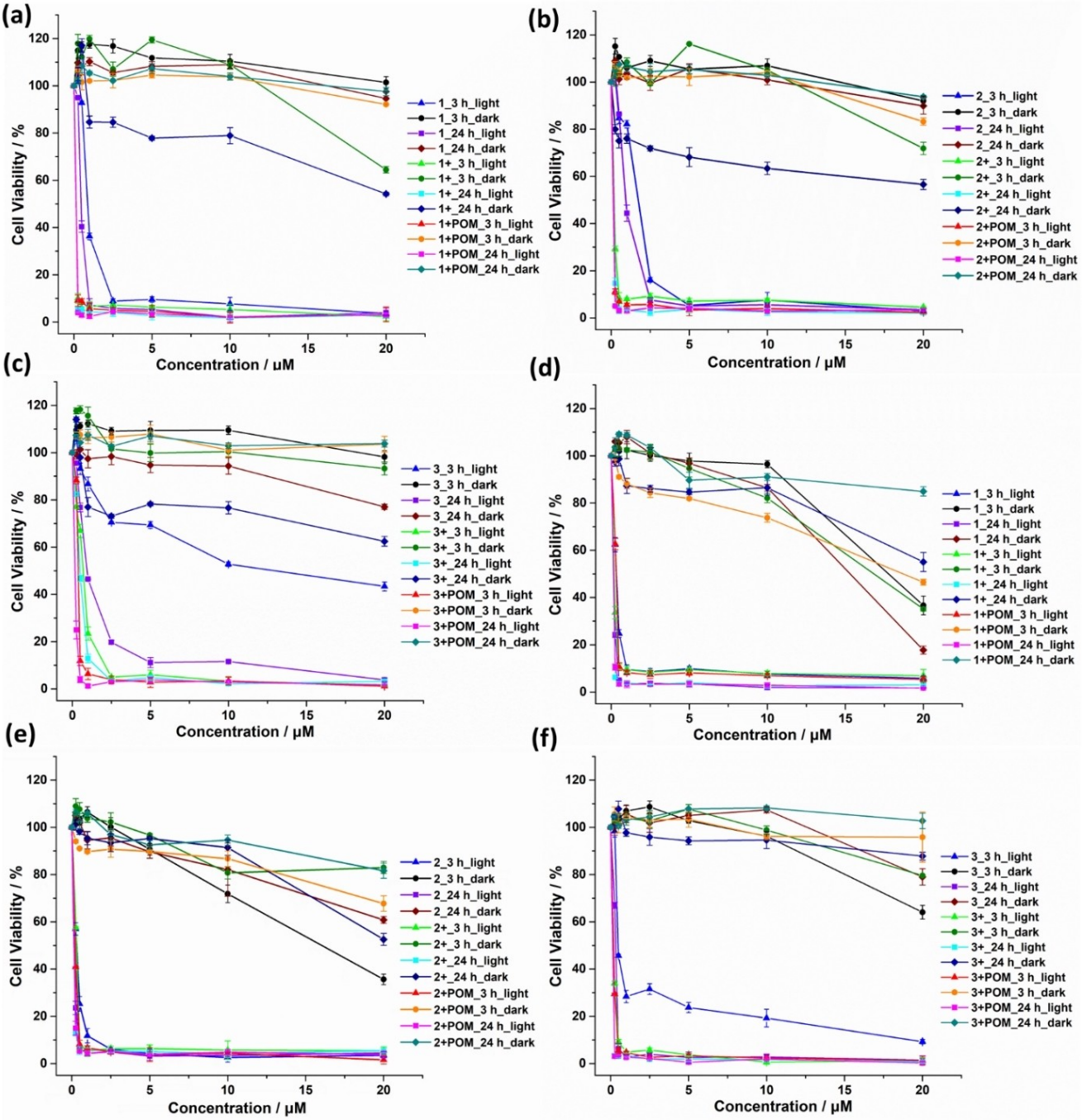

Figure 9. Cell viability for photocytotoxicity (light dose of 2 J cm^{-2}) and dark cytotoxicity of (a) and (d) **1**, **1+**, and **1+POM**, against A549 and HeLa cells, respectively, (b) and (e) **2**, **2+**, and **2+POM**, against A549 and HeLa cells, respectively, (c) and (f) **3**, **3+**, and **3+POM**, against A549 and HeLa cells, respectively, at concentrations of 0.25–20 μM. The cell viability percentage was determined by an MTT assay after 3 h or 24 h of incubation before (dark) and after (light) photoirradiation. Error bars represent the standard deviation of three replicate experiments.

($(C_4H_9)_4N{\cdot}Cl$), sodium molybdate ($Na_2MoO_4{\cdot}2H_2O$), sodium silicate (Na_2SiO_3), dimethyl sulfoxide (DMSO) (Samchun Chemical), dichloromethane (CH_2Cl_2), *n*-hexane, methanol (MeOH), acetone, acetonitrile, diethyl ether, ethyl acetate (EtOAc) (SK Chemical), 4-chloropyridine hydrochloride, 4-azidopyridine, copper(I) iodide (CuI), diisopropylethylamine (DIPEA), sodium azide, methyl iodide (MeI) (Sigma Aldrich Chemical), 4′,6-diamidino-2-phenylindole (DAPI), *N*,*N*-dimethylbutane-1,4-diamine, 4-aminomethyl pyridine, propargyl amine, 1,3-diphenylisobenzofuran (DPBF), methylene blue (MB) (TCI Chemical), 1-propanol, pyridine (Burdick & Jackson Chemical), EZ-View Live/Dead cell staining kit (calcein-AM (acetoxymethyl ester) and propidium iodide (PI)) (Biomax Chemical).

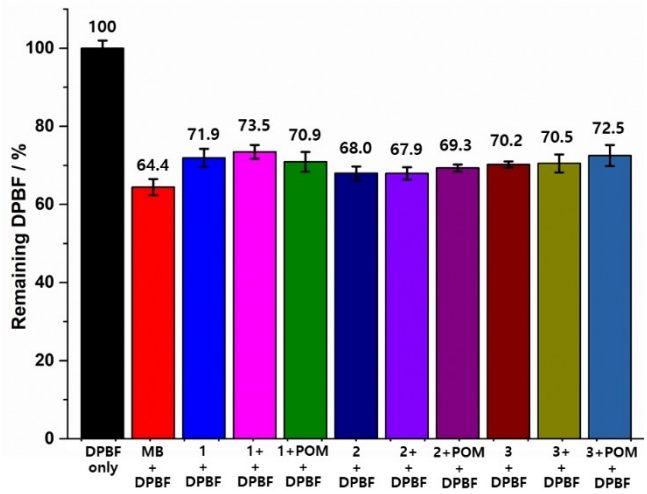

Figure 10. DPBF absorbance decay (%, 50 μM in DMSO) at 418 nm after photoirradiation (total light dose 2 J cm^{-2}; irradiation time 15 min) in the absence (control) and presence of 1 μM **1**, **1+**, **1+POM**, **2**, **2+**, **2+POM**, **3**, **3+**, **3+POM** and MB (with no tumour cells). Error bars represent the standard deviation of three replicate experiments.

General

All reactions were monitored by thin-layer chromatography (TLC) using Merck 60 silica gel F254 pre-coated (0.2 mm thickness) glass-backed sheets. Silica gel 60 A (230–400 mesh, Merck) was used for column chromatography. ^{1}H NMR spectra were obtained using a Varian spectrometer (500 MHz) at the Biohealth Products Research Centre (BPRC) of the Inje University. Chemical shifts (δ) are given in parts per million (ppm) relative to tetramethylsilane (TMS, 0 ppm). High resolution fast atom bombardment mass spectrometry (HRFABMS) analyses were conducted using a Jeol JMS700 high resolution mass spectrometer at the Daegu centre of KBSI (Korea Basic Science Institute), Kyungpook National University, Korea. UV-Vis absorption spectra were recorded on a SCINCO S-3100 UV-Vis spectrophotometer using a 1-cm quartz cuvette. IR spectra were recorded on a Varian-640 FT-IR spectrometer. Thermogravimetric analysis (TGA) was performed on a TA Instrument Q600, PH407 (Pusan KBSI).

Synthesis of Purpurin-18 Methyl Ester (P18ME)

Methyl pheophorbide-a (MPa) was prepared according to a literature procedure.[55] P18ME was synthesized as follows.[67] MPa (1 g) was dissolved in pyridine (5 mL) and diethyl ether (400 mL), followed by the addition of KOH in 1-propanol (12 g dissolved in 80 mL). Subsequently, air was bubbled into the solution for 3 h. The reaction mixture was extracted with water (500 mL); the aqueous layer was collected and its pH was adjusted to 2 with cold H_2SO_4 solution (25%). The acidified phase was then extracted with CH_2Cl_2/H_2O. Evaporation of the organic layer afforded a purple residue, which was crystallized from CH_2Cl_2/*n*-hexane, washed with water until neutral, and air-dried overnight to furnish the crude purpurin-18 carboxylic acid (500 mg, 50%, purple powder). This product was then reacted with diazomethane to produce crude P18ME, which was chromatographed on silica gel using 2% acetone/CH_2Cl_2 as an eluent to afford the title compound after crystallization from CH_2Cl_2/*n*-hexane (410 mg, 80%, purple red crystals). Mp: 267 °C. UV-Vis (CH_2Cl_2) λ_{max} ($\varepsilon\times10^4$): 412 nm (6.22), 488 nm (0.92), 509 nm (1.33), 547 nm (3.02), 644 nm (1.43), 700 nm (4.74). ^{1}H NMR (500 MHz, $CDCl_3$): δ 9.63, 9.40, 8.59 (all s and 1H, 10-H, 5-H, and 20-H, respectively), 7.91 (dd, J = 18.1, 11.7 Hz, 1H, 3^{1}CH=CH$_2$), 6.34 (d, J = 18.1, 1.1 Hz, 1H, 3^2-H), 6.22 (d, J = 11.7, 1.1 Hz, 1H, 3^2-H), 5.21 (dd, J = 9.4, 2.5 Hz, 1H, 17-H), 4.42 (q, J = 7.9 Hz, 1H, 18-H), 3.82 (s, 3H, 12-CH_3), 3.67 (q, J = 7.9 Hz, 2H, 8^1-CH_2), 3.61 (s, 3H, 17^2-OCH_3), 3.37 (s, 3H, 2-CH_3), 3.19 (s, 3H, 7-CH_3), 2.77–2.73 (m, 1H, 17^2-CH_2), 2.52–2.44 (m, 2H, 17^1-H), 2.05–1.99 (m, 1H, 17^2-CH_2), 1.77 (d, J = 7.6 Hz, 3H, 18-CH_3), 1.69 (t, J = 7.6 Hz, 3H, 8^2-CH_3), 0.28, −0.03 (all br s and 1H, NH).

Synthesis of *N*-Propargyl Purpurinimide Methyl Ester (NPPME)

P18ME (500 mg, 0.864 mmol) and propargyl amine (1 mL, 15.6 mmol, > 18 eq. excess) were dissolved in CH_2Cl_2 (5 mL), and the mixture was stirred at room temperature for 24 h. The disappearance of the 700 nm band and the appearance of a new 668 nm band in the UV-Vis spectrum indicated completion of the reaction and was used to monitor its progress. The solvents and excess propargyl amine were removed under reduced pressure. The residue was redissolved in CH_2Cl_2 (5 mL) and mixed with a solution of diazomethane in diethyl ether was added and the mixture stirred for 5 min. The reaction mixture was treated with a catalytic amount of methanolic KOH at room temperature for 3–5 min, diluted with 200 mL of CH_2Cl_2, and immediately washed with 2×400 mL water. The organic layer was dried over anhydrous sodium sulfate, filtered, and evaporated to afford the crude product, which was chromatographed on a silica column eluting with 2% acetone/CH_2Cl_2 to give the desired compound NPPME (372 mg, 70%). UV-Vis (CH_2Cl_2) λ_{max} ($\varepsilon\times10^4$): 412 nm (6.03), 481 nm (1.28), 511 nm (1.63), 551 nm (3.26), 658 nm (1.67), 707 nm (4.93). ^{1}H-NMR (500 MHz, $CDCl_3$): δ 9.63, 9.37, 8.56 (all s and 1H, 10-H, 5-H and 20-H), 7.91 (dd, J = 18.1, 11.7 Hz, 1H, 3^{1}CH=CH$_2$), 6.31 (d, J = 18.0, 1.1 Hz, 1H, 3^2-H), 6.18 (d, J = 11.8, 1.1 Hz, 1H, 3^2-H), 5.41–5.36 (dd, J = 9.3, 2.4 Hz, 1H, 17-H), 5.35–5.32, 5.31–5.23 (all m and 1H, N-C$\underline{H_2}$-alkyne), 4.36 (q, J = 6.0 Hz, 1H, 18-H), 3.84 (s, 3H, 12-CH_3), 3.66 (m, 2H, 8^1-CH_2), 3.57 (s, 3H, OCH_3), 3.35 (s, 3H, 2-CH_3), 3.17 (s, 3H, 7-CH_3), 2.81–2.70 (m, 1H, 17^2-CH_2), 2.47–2.39 (m, 2H, 17^1-H), 2.09–1.97 (s, 1H, 17^2-CH_2), 2.31 (t, J = 2.4 Hz, 1H, C≡CH), 1.74 (d, J = 6.0 Hz, 3H, 18-CH_3), 1.62 (t, J = 7.6 Hz, 3H, 8^2-CH_3), 0.11, 0.07 (all br s and 1H, NH).

Preparation of 4-Azidopyridine

4-Chloropyridine hydrochloride (50 mg) and sodium azide (1 g) were dissolved in H_2O (50 mL), and the solution was stirred at room temperature for 24 h. The reaction mixture was extracted with diethyl ether/H_2O. The organic layer was dried over anhydrous sodium sulfate, filtered, and evaporated to obtain a yellow oil (350 mg, 70%).

Preparation of POM 4[36,56]

To a solution of $Na_2MoO_4\cdot2H_2O$ (29.03 g, 0.12 mol) in H_2O (120 mL) was slowly added HNO_3 (13 M, 37 mL), followed by a solution of Na_2SiO_3 (1.3 g, 0.0107 mol) in H_2O (50 mL). The resulting yellow solution was heated at 80 °C for 30 min, the above period of time being required for the transformation of the β-form of $[SiMo_{12}O_{40}]^{4-}$ into the α-isomer. The reaction mixture was treated with a solution of $(C_4H_9)_4N\cdot Cl$ in H_2O (10 mL) at room temperature to allow the formation of a homogeneous solution in the preparation of POM complexes containing the each CPI, which is soluble in the organic solvent system. The yellow precipitate was filtered off, washed with water and ethanol, and dried in air at room temperature to furnish the target product **4** (20.1 g, 68%). UV-Vis (DMSO) λ_{max} ($\varepsilon\times10^4$): 291 nm (6.37). FTIR (ATR (attenuated total reflectance)) 943, 897, 791 cm^{-1}.

Synthesis of Purpurin-18-*N*-(*N,N*-dimethylbutyl)imide Methyl Ester 1

The same method for the synthesis of NPPME except use of the corresponding amine (*N,N*-dimethylbutane-1,4-diamine, 1.80 mmol, >10 eq. excess) with P18ME (100 mg, 0.173 mmol) was carried out. The reaction mixture was chromatographed on a silica gel using 10% MeOH/CH_2Cl_2 as an eluent to furnish the target product **1** (82 mg, 70%). UV-Vis (DMSO, nm) (log ε): 421 (4.67), 514 (4.29), 553 (4.36), 651 (4.04), 707 (4.40). ^{1}H-NMR (500 MHz, $CDCl_3$): δ 9.51 (s, 1H, 10-H), 9.27 (s, 1H, 5-H), 8.50 (s, 1H, 20-H), 7.86–7.80 (dd, J=17.9, 11.5 Hz, 1H, 3^{1}CH=CH$_2$), 6.24–6.20 (dd, J=17.8, 1.1 Hz, 1H, 3^2-H), 6.10–6.08 (dd, J=11.5, 1.1 Hz, 1H, 3^2-H), 5.27–5.24 (dd, J=9.2, 2.8 Hz, 1H, 17-H), 4.41 (t, J=7.5 Hz, 2H, N^1), 4.30 (q, J=7.9 Hz, 1H, 18-H), 3.87–3.77 (m, 2H, N^4), 3.72 (s, 3H, 12-CH$_3$), 3.58 (q, J=7.6 Hz, 2H, 8^1-CH$_2$), 3.28 (s, 3H, OCH$_3$), 3.08 (s, 3H, 2-CH$_3$), 2.93 (br, 3H, 7-CH$_3$), 2.64–2.58 (m, 6H, N^5), 2.38–2.32 (m, 1H, 17^2-CH$_2$), 2.28–2.22 (m, 1H, 17^2-CH$_2$), 1.98 (m, 2H, 17^1-CH$_2$), 1.91 (m, 2H, N^3), 1.69 (d, J=7.5 Hz, 3H, 18-CH$_3$), 1.58 (t, J=7.7 Hz, 3H, 8^2-CH$_3$), 1.46–1.38 (m, 7.5 Hz, 2H, N^2), −0.06, −0.15 (all br s and 1H, NH). HRFABMS: Calcd. for $C_{40}H_{49}N_6O_4$ [M+H]$^+$ 677.3815; Found 677.3818.

Preparation of Purpurin-18-*N*-(*N,N,N*-trimethylammonium iodide-butyl)imide Methyl Ester 1+

Purpurinimide **1** (28 mg, 0.041 mmol) and MeI (1.5 mL, >500 eq. excess) were dissolved in CH_2Cl_2 (5 mL), and the solution was stirred at room temperature under N_2 for 24 h. The solvent and excess MeI were removed under reduced pressure, affording the title compound **1+** in quantitative yield as a purple red solid without further purification. UV-Vis (DMSO, nm) (log ε): 421 (4.84), 481 (4.29), 512 (4.33), 551 (4.61), 648 (4.33), 707 (4.78). ^{1}H-NMR (500 MHz, $CDCl_3$): δ 9.37 (s, 1H, 10-H), 9.23 (s, 1H, 5-H), 8.48 (s, 1H, 20-H), 7.84–7.78 (dd, J=17.9, 11.4 Hz, 1H, 3^{1}CH=CH$_2$), 6.24 (d, J=17.8 Hz, 1H, 3^2-H), 6.11 (d, J=11.6 Hz, 1H, 3^2-H), 5.22–5.20 (d, J=9.1 Hz, 1H, 17-H), 4.46 (t, J=7.5 Hz, 2H, N^1), 4.32–4.24 (m, 1H, 18-H), 3.84–3.79 (m, 1H, N^4), 3.79–3.69 (m, 1H, N^4), 3.61 (s, 3H, 12-CH$_3$), 3.52 (m, 2H, 8^1-CH$_2$), 3.46 (s, 3H, OCH$_3$), 3.41 (s, 9H, N^5), 3.28 (s, 3H, 2-CH$_3$), 3.03 (s, 3H, 7-CH$_3$), 2.66–2.59 (m, 1H, 17^2-CH$_2$), 2.35–2.25 (m, 2H, 17^1-CH$_2$), 2.23 (m, 1H, 17^2-CH$_2$), 1.90–1.75 (m, 2H, N^3), 1.69 (d, J=7.6 Hz, 3H, 18-CH$_3$), 1.54 (t, J=7.1 Hz, 3H, 8^2-CH$_3$), 1.44 (m, 2H, N^2), 0.12, −0.12 (all s and 1H, NH). HRFABMS: Calcd. for $C_{41}H_{51}N_6O_4$ [M-I]$^+$ 691.3966; Found 691.3977.

Preparation of Purpurin-18-*N*-(*N,N,N*-trimethyl ammonium) butyl-imide Methyl Ester-POM Complex 1+POM

A mixture of CPI **1+** (33 mg, 0.04 mmol) and Keggin-type POM **4** (α-(Bu$_4$N)$_4$[SiMo$_{12}$O$_{40}$]) (28 mg, 0.01 mmol) in acetonitrile (7 mL) was stirred at room temperature for 24 h. The resulting dark green precipitate was filtered off, washed with cold acetonitrile for several times, and dried to afford the target product **1+POM** (34 mg, 73%) without further purification. UV-Vis (DMSO, nm) (log ε): 421 (4.75), 513 (4.07), 553 (4.30), 649 (4.10), 707 (4.51). ^{1}H-NMR (500 MHz, DMSO-d$_6$): δ 9.52 (br, 1H, 10-H), 9.37 (br, 1H, 5-H), 8.91 (s, 1H, 20-H), 8.17–8.11 (dd, J=18.3, 12.0 Hz, 1H, 3^{1}CH=CH$_2$), 6.42 (d, J=17.6 Hz, 1H, 3^2-H), 6.20 (d, J=11.5 Hz, 1H, 3^2-H), 5.27 (d, J=8.5 Hz, 1H, 17-H), 4.50 (q, J=7.2 Hz, 1H, 18-H), 4.45–4.36 (m, 2H, N^1), 3.76–3.71 (m, 1H, N^4), 3.67 (s, 3H, 12-CH$_3$), 3.65–3.61 (m, 1H, N^4), 3.51 (m, 2H, 8^1-CH$_2$), 3.39 (3H, OCH$_3$ & 3H, 2-CH$_3$, overlapped with DMSO solvent), 3.13 (s, 9H, N^5), 3.06 (s, 3H, 7-CH$_3$), 2.62–2.54 (m, 1H, 17^2-CH$_2$), 2.35–2.28 (m, 2H, 17^1-CH$_2$), 1.98 (m, 1H, 17^2-CH$_2$), 1.91 (m, 2H, N^3), 1.73 (d, J=7.7 Hz, 3H, 18-CH$_3$), 1.51 (t, J=7.2 Hz, 3H, 8^2-CH$_3$), 1.33–1.19 (m, 2H, N^2), −0.36, −0.45 (all br s and 1H, NH). FTIR (ATR) 941, 899, 792 cm^{-1}.

Synthesis of Purpurin-18-*N*-(pyridine-4-ylmethyl)imide Methyl Ester 2[68]

The same method for the synthesis of NPPME except use of the corresponding amine (4-aminomethyl pyridine, 1.80 mmol, >10 eq. excess) with P18ME (100 mg, 0.173 mmol) was carried out. The reaction mixture was chromatographed on a silica gel using 50% EtOAc/n-Hx as an eluent to furnish the target product **2** (98 mg, 85%). UV-Vis (DMSO, nm) (log ε): 421 (4.72), 512 (4.19), 551 (4.31), 665 (3.62), 707 (4.40). ^{1}H-NMR (500 MHz, $CDCl_3$): δ 9.54, 9.28, 8.49 (each s and 1H, 10-H, 5-H, 20-H), 8.53 (m, 2H, N^3), 7.85 (dd, J=17.5, 11.3 Hz, 1H, 3^1-H), 7.52 (d, J=4.8 Hz, 2H, N^2), 6.24 (dd, J=17.9, 1.1 Hz, 1H, 3^2-H), 6.11 (dd, J=11.6, 1.1 Hz, 1H, 3^2-H), 5.62 (s, 2H, N^1), 5.26 (d, J=9.1 Hz, 1H, 17-H), 4.27 (q, J=7.6 Hz, 1H, 18-H), 3.74 (s, 3H, 12-CH$_3$), 3.58 (q, J=7.8 Hz, 2H, 8^1-CH$_2$), 3.47 (s, 3H, OCH$_3$), 3.27 (s, 3H, 2-CH$_3$), 3.09 (s, 3H, 7-CH$_3$), 2.64–2.55 (m, 1H, 17^2-CH$_2$), 2.35–2.25 (m, 2H, 17^1-CH$_2$), 2.06 (m, 1H, 17^2-CH$_2$), 1.68 (d, J=7.3 Hz, 3H, 18^1-CH$_3$), 1.60 (t, J=7.7 Hz, 3H, 8^2-CH$_3$), 0.07, −0.06 (each br s, each 1H, NH). HRFABMS: Calcd. for $C_{40}H_{41}N_6O_4$ [M+H]$^+$ 669.3189; Found 669.3192.

Preparation of Purpurin-18-*N*-(1-methylpyridinium iodide-4-yl-methyl)-imide Methyl Ester 2+[69]

Purpurinimide **2** (27 mg, 0.041 mmol) and MeI (1.5 mL, >500 eq. excess) were dissolved in CH_2Cl_2 (5 mL), and the solution was stirred at room temperature under N_2 for 24 h. The solvent and excess MeI were removed under reduced pressure, affording the title compound **2+** in quantitative yield as a purple red solid without further purification. UV-Vis (DMSO, nm) (log ε): 419 (4.84), 481 (4.32), 512 (4.32), 551 (4.51), 651 (4.28), 707 (4.59). ^{1}H-NMR (500 MHz, $CDCl_3$): δ 9.16 (br d, J=6.2 Hz, 1H, N^3, pyridine), 9.12, 9.10, 8.45 (each s and 1H, 10-H, 5-H, 20-H), 8.20 (br d, J=6.2 Hz, 2H, N^2, pyridine), 7.82–7.76 (dd, J=17.9, 11.5 Hz, 1H, 3^{1}CH=CH$_2$), 6.24 (d, J=17.9 Hz, 1H, 3^2-H), 6.12 (d, J=11.5 Hz, 1H, 3^2-H), 5.81–5.70 (m, 2H, N^1), 5.15 (d, J=8.7 Hz, 1H, 17-H), 4.61 (s, 3H, N^4, pyridine-C$\underline{H}_3$), 4.26 (q, J=7.4 Hz, 1H, 18-H), 3.85–3.79 (m, 1H, 8^1-H), 3.78–3.72 (m, 1H, 8^1-H), 3.66 (s, 3H, 12-CH$_3$, overlapped with solvent), 3.48 (s, 3H, OCH$_3$), 3.27 (s, 3H, 2-CH$_3$), 2.92 (s, 3H, 7-CH$_3$), 2.60-2.53 (m, 1H, 17^2-CH$_2$), 2.29–2.19 (m, 2H, 17^1-CH$_2$), 2.00–1.92 (m, 1H, 17^2-CH$_2$), 1.73 (d, J=7.3 Hz, 3H, 18-CH$_3$), 1.43 (t, J=7.3 Hz, 3H, 8^2-CH$_3$), 0.03, 0.01 (all br s and 1H, NH). HRFABMS: Calcd. for $C_{41}H_{43}N_6O_4$ [M-I]$^+$ 683.3340; Found 683.3342.

Preparation of Purpurin-18-*N*-(1-methylpyridinium iodide-4-yl-methyl)-imide Methyl Ester-POM Complex 2+POM

A mixture of CPI **2+** (32 mg, 0.04 mmol) and Keggin-type POM **4** (α-(Bu$_4$N)$_4$[SiMo$_{12}$O$_{40}$]) (28 mg, 0.01 mmol) in acetonitrile (7 mL) was stirred at room temperature for 24 h. The resulting dark green precipitate was filtered off, washed with cold acetonitrile for several times, and dried to afford **2+POM** (32 mg, 70%) without further purification. UV-Vis (DMSO, nm) (log ε): 421 (4.75), 481 (4.10), 514 (4.11), 551 (4.50), 649 (4.14), 707 (4.63). ^{1}H-NMR (500 MHz, DMSO-d$_6$): δ 9.80, 9.55, 8.99 (each s and 1H, 10-H, 5-H, 20-H), 8.99 (br, 2H, N^3, pyridine, overlapped with 20-H), 8.39 (br d, J=6.6 Hz, 2H, N^2, pyridine), 8.28–8.22 (m, 1H, 3^{1}CH=CH$_2$), 6.51 (d, J=17.9 Hz, 1H, 3^2-H), 6.29 (dd, J=11.6 Hz, 1H, 3^2-H), 5.91–5.83 (m, 2H, N^1), 5.21 (m, 1H, 17-H), 4.53 (m, 1H, 18-H), 4.39 (s, 3H, N^4, pyridine-C$\underline{H}_3$), 3.82 (s, 3H, 12-CH$_3$), 3.73 (m, 2H, 8^1-H), 3.45 (3H, OCH$_3$, overlapped with DMSO solvent), 3.31 (s, 3H, 2-CH$_3$), 3.21 (s, 3H, 7-CH$_3$), 2.55 (m, 1H, 17^2-CH$_2$, overlapped with DMSO solvent), 2.35 (m, 2H, 17^1-CH$_2$), 2.18 (m, 1H, 17^2-CH$_2$), 1.76 (d, J=7.6 Hz, 3H, 18-CH$_3$), 1.65 (t, J=7.7 Hz, 3H, 8^2-CH$_3$), 0.11, −0.06 (all br s and 1H, NH). FTIR (ATR) 941, 899, 792 cm^{-1}.

Synthesis of Purpurin-18-*N*-(1-(Pyridin-4-yl)-1,2,3-triazol-4-ylmethyl)-imide Methyl Ester 3

A solution of NPPME (50 mg, 0.081 mmol, 1 eq.), 4-azidopyridine (0.10 mmol, 1.2 eq. per C≡CH group), DIPEA (4 mol% per C≡CH group), CuI (2 mol% per C≡CH group), and AcOH (4 mol% per C≡CH group) in CH_2Cl_2 (5 mL) was stirred at room temperature for 0.5–1 h. The reaction mixture was chromatographed on a silica plate (preparative thin layer chromatography) using 2% MeOH/CH_2Cl_2 as an eluent to furnish the target product **3** (42 mg, 70%). UV-Vis (DMSO, nm) (log ε): 421 (4.73), 481 (4.05), 512 (4.04), 551 (4.26), 649 (3.94), 707 (4.43). ^{1}H-NMR (500 MHz, $CDCl_3$): δ 9.53, 9.29, 8.49 (each s and 1H, 10-H, 5-H, 20-H), 8.66 (br d, J=5.7 Hz, 2H, N^4, pyridine), 8.43 (s, 1H, N^2, 5-triazole), 7.86–7.80 (dd, J=17.7, 11.7 Hz, 1H, 3^{1}CH=CH$_2$), 7.76 (d, J=6.1 Hz, 2H, N^3, pyridine), 6.24 (d, J=17.9 Hz, 1H, 3^2-H), 6.11 (d, J=11.9 Hz, 1H, 3^2-H), 5.96 (d, J=14.9 Hz, 1H, N^1), 5.73 (d, J=14.8 Hz, 1H, N^1), 5.33–5.31 (dd, J=8.7, 2.4 Hz, 1H, 17-H), 4.28 (q, J=7.4 Hz, 1H, 18-H), 3.76 (s, 3H, 12-CH$_3$), 3.58 (q, J=7.4 Hz, 2H, 8^1-CH$_2$), 3.50 (s, 3H, OCH$_3$), 3.28 (s, 3H, 2-CH$_3$), 3.09 (s, 3H, 7-CH$_3$), 2.71–2.66 (m, 1H, 17^2-CH$_2$), 2.41–2.26 (m, 2H, 17^1-CH$_2$), 1.91–1.85 (m, 1H, 17^2-CH$_2$), 1.70 (d, J=7.2 Hz, 3H, 18-CH$_3$), 1.59 (t, J=7.6 Hz, 3H, 8^2-CH$_3$), 0.02, −0.10 (all br s and 1H, NH). HRFABMS: Calcd. for $C_{42}H_{42}N_9O_4$ $[M+H]^+$ 736.3360; Found 736.3357.

Preparation of Purpurin-18-*N*-(1-(1-methylpyridinium iodide-4-yl)-1,2,3-triazol-4-ylmethyl)imide Methyl Ester 3+

Clicked purpurinimide **3** (30 mg, 0.041 mmol) and MeI (1.5 mL, >500 eq. excess) were dissolved in CH_2Cl_2 (5 mL), and the solution was stirred at room temperature under N_2 for 24 h. The solvent and excess MeI were removed under reduced pressure, affording the title compound **3+** in quantitative yield as a purple red solid without further purification. UV-Vis (DMSO, nm) (log ε): 421 (4.68), 512 (4.02), 551 (4.17), 707 (4.34). ^{1}H-NMR (500 MHz, $CDCl_3$): δ 8.94 (br, 3H, 10-H, 5-H, 20-H, all overlapped), 8.74 (br, 2H, N^4, pyridine), 8.48 (s, 1H, N^2, 5-triazole), 8.31 (br, 2H, N^3, pyridine), 7.77 (br m, 1H, 3^{1}CH=CH$_2$), 6.23 (d, J=17.1 Hz, 1H, 3^2-H), 6.10 (d, J=10.7 Hz, 1H, 3^2-H), 5.83 (br, 1H, N^1), 5.64 (br, 1H, N^1), 5.28 (br, 1H, 17-H), 4.26 (br, 1H, 18-H), 4.11 (br s, 3H, N^5, pyridine-C<u>H</u>$_3$), 3.56 (s, 3H, 12-CH$_3$), 3.42 (m, 2H, 8^1-H), 3.28 (br s, 6H, OCH$_3$ + 2-CH$_3$, overlapped), 2.69 (br, 4H, 7-CH$_3$ + 17^2-CH$_2$), 2.49–2.38 (m, 2H, 17^1-CH$_2$), 1.97 (m, 1H, 17^2-CH$_2$), 1.82 (br, 3H, 18-CH$_3$), 1.53 (3H, 8^2-CH$_3$, overlapped with solvent), −0.55 (br and 2H, NH). HRFABMS: Calcd. for $C_{43}H_{44}N_9O_4$ $[M-I]^+$ 750.3511; Found 750.3513.

Preparation of Purpurin-18-*N*-(1-(1-methylpyridinium iodide-4-yl)-1,2,3-triazol-4-ylmethyl)imide Methyl Ester-POM Complex 3+POM

A mixture of clicked CPI **3+** (35 mg, 0.04 mmol) and Keggin-type POM **4** (α-(Bu$_4$N)$_4$[SiMo$_{12}$O$_{40}$]) (28 mg, 0.01 mmol) in acetonitrile (7 mL) was stirred at room temperature for 24 h. The resulting dark green precipitate was filtered off, washed with cold acetonitrile for several times, and dried to afford **3+POM** (36 mg, 75%) without further purification. UV-Vis (DMSO, nm) (log ε): 421 (4.78), 479 (4.22), 511 (4.23), 552 (4.52), 651 (4.29), 707 (4.69). ^{1}H-NMR (500 MHz, DMSO-d$_6$): δ 9.48, 9.35, 9.31 (each br or s and 1H, 10-H, 5-H, 20-H), 9.10 (br d, J=6.3 Hz, 2H, N^4, pyridine), 8.91 (s, 1H, N^2, 5-triazole), 8.66 (br d, J=6.6 Hz, 2H, N^3, pyridine), 8.12 (br m, 1H, 3^{1}CH=CH$_2$), 6.40 (d, J=17.6 Hz, 1H, 3^2-H), 6.20 (d, J=11.7 Hz, 1H, 3^2-H), 5.76 (br m, 2H, N^1), 5.24 (br d, J=8.6 Hz, 1H, 17-H), 4.48 (br q, J=7.0 Hz, 1H, 18-H), 4.32 (s, 3H, N^5, pyridine-C<u>H</u>$_3$), 3.64 (s, 3H, 12-CH$_3$), 3.40 (br, 2H, 8^1-H & 3H, OCH3 & 3H, 2-CH$_3$, overlapped with DMSO solvent), 3.04 (s, 3H, 7-CH$_3$), 2.64-2.55 (m, 1H, 17^2-CH$_2$), 2.42–2.36 (m, 1H, 17^1-CH$_2$), 2.29 (m, 1H, 17^1-CH$_2$), 1.97–1.91 (m, 1H, 17^2-CH$_2$), 1.74 (d, J=6.9 Hz, 3H, 18-CH$_3$), 1.50 (br t, J=6.2 Hz, 3H, 8^2-CH$_3$), −0.28, −0.39 (all br s and 1H, NH). FTIR (ATR) 941, 899, 792 cm^{-1}.

Cell Culture and Photoirradiation

The tested cell lines were A549 human lung carcinoma and HeLa human cervical cells obtained from the cell line bank of Seoul National University cancer research center, and were grown in medium RPMI-1640 (Sigma-Aldrich) with 10% fetal bovine serum, glutamine, and 1% penicillin at 37 °C in a humidified atmosphere of 5% CO_2 in air. Phosphate buffer saline (PBS, Sigma-Aldrich), optical microscope (Olympus, CK40-32 PH), ELISA (enzyme linked immunosorbent assay)-reader (BioTek, SynergyHT), trypsin-EDTA (ethylenedia-minetetraacetic acid) solution (Sigma-Aldrich), and incubator (37 °C, 5% CO_2) were used. PDT was carried out using a diode laser apparatus (BioSpec LED, Russia) equipped with a halogen lamp, a band-pass filter (640–710 nm), and a fiber optics bundle. The duration of irradiation in PDT treatment was calculated taking into account the empirically determined effective dose of light energy (total light dose of 2 J cm^{-2}, irradiation time 15 min).

MTT assay and cell viability

Cells from each cell line were placed in a 48-well, flat-bottomed microplate at a volume of 200 μL (2×10^4 cells/well) for stationary culture. After 24 h of incubation, the medium was removed, the cultures were washed twice with physiological saline, and purpurinimides **1–3**, CPIs **1+**–**3+**, and their CPI–POM complexes **1+POM**, **2+POM** and **3+POM** (constant concentration of each PI and CPI) in 200 μL of the mixed medium were added to each well. After 24 h of incubation, the solutions were discarded, and the cultures were washed 3 times with physiological saline, followed by the addition of medium (200 μL/well). The cultures were then irradiated (2 J cm^{-2}) from a distance of 20 cm for 15 min, followed by an MTT (3-(4,5-dimethylthiazol-2-yl)-2,5-diphenyltetrazolium bromide) assay to evaluate their response to PDT. In the assay, MTT solution (EZ-CYTOX, DOGEN, 10 μL) was added to each cell culture well followed by culturing in an incubator for 1 h. Detergent solution (TACS™, Trevigen, 200 μL) was added to the culture, shaken for 10 min, and the absorbance was measured with an ELISA-reader at 570 nm. Measurements were performed after 12 h and 24 h of incubation after photoirradiation. Each group consisted of 3 wells.

Cellular accumulation study

A549 cells or HeLa cells were seeded in confocal dishes at a density of 2×10^4 cells/dish. After 24 h of incubation, the medium was removed, and the dishes were washed twice with PBS. Subsequently, purpurinimides **1–3**, CPIs **1+**–**3+**, and their CPI–POM complexes **1+POM**, **2+POM** and **3+POM** solution of 5 μM concentration were added to each dish. After 24 h of incubation, the cells were washed with PBS and fixed with 4% formalin (Sigma-Aldrich) for 30 min. The fixed cells were washed again with PBS. Samples were also stained with DAPI (200 nM) (BioLegend) or Mitoorange (500 nM) to identify the site of the nucleus or mitochondria in the cells. Cellular uptake images were recorded using a confocal laser scanning microscope (CLSM, LSM 510 META, Germany) at Inje University.

Singlet oxygen photogeneration study

DPBF was used as a selective singlet oxygen ($^1O_2$) acceptor, being bleached upon reaction with $^1O_2$.[63] Five sample solutions of DPBF

in DMSO (50 μM) containing, respectively, DPBF only (50 μM, control sample), DPBF + MB (1 μM), DPBF + purpurinimides **1**–**3** (1 μM), DPBF + CPIs **1**+ –**3**+ (1 μM), DPBF + CPI–POM complexes **1**+**POM**, **2**+**POM** and **3**+**POM** (1 μM) were prepared in the dark. All samples were placed in a 96-well plate and covered with aluminum foil. The samples were irradiated (2 J cm^{-2}) for 15 min. After irradiation, visible spectra of the sample solutions were recorded, and the normalized absorbances of DPBF at 418 nm were reported. The $^1O_2$ photogeneration activities of all compounds were compared based on the different absorbance decay of each sample relative to that of the DPBF control sample.

Morphological changes induced by PDT

A549 cells were seeded in a 48-well plate at a density of 2× 10^4 cells/well and incubated for 24 h (37 °C, 5% CO_2). And 5 μM of **3**, **3**+, and **3**+**POM** in 200 μL of the mixed medium was added in each well. After 24 h of incubation, the mixed solution in each well was discarded. And the cells were washed with PBS (200 μL×3), and 200 μL of the mixed medium was added. The cells were irradiated with the LED (2 J cm^{-2}) for 15 min, and incubated for 24 h. The images of morphological changes were obtained by an optical microscopy (Olympus, CK40-32 PH, Japan), and compared with those in the cells with no irradiation.

Cell Live/Dead Image Study

A549 cells were seeded in cell culture slide at a density of 2× 10^4 cells/slide. After 24 h of incubation, the medium was removed, and the dishes were washed three times with PBS. Thereafter, 1 μM of **3**, **3**+, and **3**+**POM** were added to the dishes, respectively. After 24 h of incubation, the slide was irradiated (2 J cm^{-2}) for 15 min and incubated for 24 h. The viability of cells subjected to phototherapy was visualized using a double staining procedure with calcein-AM and PI, generating green fluorescence from calcein-AM (live cells) and red fluorescence from PI (dead cells). The staining solution composed of 10 μL calcein-AM (1 mmol/DMSO) and 15 μL PI (1.5 mmol/water) in 5 mL PBS was added to each well, followed by incubation in the dark for 30 min. Images of live/dead cell were recorded using a fluorescence microscope (Axioskope2 Plus, Germany).

Acknowledgements

This research was supported by Basic Science Research Program through the National Research Foundation of Korea (NRF) funded by the Ministry of Education (NRF-2020R1I1A1A01060632) and the Korea government (MSIT) (NRF-2017R1A2B4010615 and NRF-2020R1F1A1070571).

Conflict of Interest

The authors declare no conflict of interest.

Keywords: Photodynamic therapy · Photosensitizer · Polyoxometalate · Purpurinimide · Supramolecular complex

[1] A. Nazarova, A. Ignatova, A. Feofanov, T. Karmakova, A. Pljutinskaya, O. Mass, M. Grin, R. Yakubovskaya, A. Mironov, J. C. Maurizot, *Photochem. Photobiol. Sci.* **2007**, *6*, 1184–1196.
[2] H. Taima, A. Okubo, N. Yoshioka, H. Inoue, *Chem. Eur. J.* **2006**, *12*, 6331–6340.
[3] S. Mettath, B. R. Munson, R. K. Pandey, *Bioconjugate Chem.* **1999**, *10*, 94–102.
[4] T. Uno, K. Hamasaki, M. Tanigawa, S. Shimabayashi, *Inorg. Chem.* **1997**, *36*, 1676–1683.
[5] J. Z. Li, J. J. Wang, I. Yoon, B. C. Cui, Y. K. Shim, *Bioorg. Med. Chem. Lett.* **2012**, *22*, 1846–1849.
[6] M. Wainwright, *Anti-Cancer Agents Med. Chem.* **2008**, *8*, 280–291.
[7] R. Bonnett, *Chem. Soc. Rev.* **1995**, *24*, 19–33.
[8] E. S. Nyman, P. H. Hynninen, *J. Photochem. Photobiol. B* **2004**, *73*, 1–28.
[9] H. C. Kolb, M. G. Finn, K. B. Sharpless, *Angew. Chem. Int. Ed.* **2001**, *40*, 2004–2012; *Angew. Chem.* **2001**, *113*, 2056–2075.
[10] C. W. Tornøe, M. Meldal, M. Lebl, R. A. Houghten, *The Wave of the Future*, Peptidotriazoles: Copper(I)-Catalyzed 1, 3-Dipolar Cycloadditions on Solid-Phase.American Peptide Society and Kluwer Academic Publishers: San Diego, 2001; 263–264.
[11] C. W. Tornøe, C. Christensen, M. Meldal, *J. Org. Chem.* **2002**, *67*, 3057–3064.
[12] V. V. Rostovtsev, L. G. Green, V. V. Fokin, K. B. Sharpless, *Angew. Chem. Int. Ed.* **2002**, *41*, 2596–2599; *Angew. Chem.* **2002**, *114*, 2708–2711.
[13] R. Bonnet, *Chemical Aspects of Photodynamic Therapy*, Gordon and Breach Science Publishers: Netherlands, 2000.
[14] R. K. Pandey, G. Zheng, K. M. Kadish, K. M. Smith, R. Guilard, *The Porphyrin Handbook*, Vol. 6, Academic Press: New York, 2000, 157–230.
[15] R. K. Pandey, L. N. Goswami, Y. Chen, A. Gryshuk, J. R. Missert, A. Oseroff, T. J. Dougherty, *Lasers Surg. Med.* **2006**, *38*, 445–467 and references therein.
[16] K. Szaciłowski, W. Macyk, A. Drzewiecka-Matuszek, M. Brindell, G. Stochel, *Chem. Rev.* **2005**, *105*, 2647–2694.
[17] B. W. Henderson, T. J. Dougherty, *Photodynamic Therapy: Basic Principles and Clinical Applications*; Marcel Dekker: New York, 1992.
[18] J. G. Moser, *Photodynamic Tumor Therapy: 2nd and 3rd Generation Photosensitizers*; Harwood Academic Publishers: Amsterdam, 1998.
[19] J. Li, X. Zhang, Y. Liu, I. Yoon, D.-K. Kim, J.-G. Yin, J.-J. Wang, Y. K. Shim, *Bioorg. Med. Chem.* **2015**, *23*, 1684–1690.
[20] J. Li, Y. Liu, X.-S. Xu, Y.-L. Li, S.-G. Zhang, I. Yoon, Y. K. Shim, J.-J. Wang, J.-G. Yin, *Org. Biomol. Chem.* **2015**, *13*, 1992–1995.
[21] K. M. Kadish, K. M. Smith, R. Guilard, I. Yoon, D. Demberelnyamba, J. Z. Li, Y. K. Shim, *Handbook of Porphyrin Science with Applications to Chemistry*, Physics, Materials Science, Engineering, Biology, and Medicine, World Scientific Publishing: Singapore, **2014**, V33, Ch. 173, Ionic Liquid-Based Chlorins and Type III Mechanism of Photodynamic Therapy (PDT), pp. 167–224.
[22] B. C. Cui, I. Yoon, J. Z. Li, W. K. Lee, Y. K. Shim, *Int. J. Mol. Sci.* **2014**, *15*, 8091–8105.
[23] I. Yoon, J. H. Kim, J. Z. Li, Y. K. Shim, *Clin. Endosc.* **2013**, *46*, 7–23.
[24] D. Pissuwan, T. Niidome, M. B. Cortie, *J. Controlled Release* **2011**, *149*, 65–71.
[25] P. Huang, J. Lin, D. Yang, C. Zhang, Z. Li, D. Cui, *J. Controlled Release* **2011**, *152*, e33–e34.
[26] G. F. Paciotti, D. G. I. Kingston, L. Tamarkin, *Drug Dev. Res.* **2006**, *67*, 47–54.
[27] M. K. K. Oo, X. Yang, H. Du, H. Wang, *Nanomedicine* **2008**, *3*, 777–786.
[28] B.-Y. Zheng, X.-M. Shen, D.-M. Zhao, Y.-B. Cai, M.-R. Ke, J.-D. Huang, *J. Photochem. Photobiol. B* **2016**, *159*, 196–204.
[29] J. Lee, J. Kim, M. Jeong, H. Lee, U. Goh, H. Kim, B. Kim, J.-H. Park, *Nano Lett.* **2015**, *15*, 2938–2944.
[30] O. Penon, T. Patiño, L. Barrios, C. Nogués, D. B. Amabilino, K. Wurst, L. Pérez-García, *ChemistryOpen* **2015**, *4*, 127–136.
[31] S. B. Kim, T. H. Lee, I. Yoon, Y. K. Shim, W. K. Lee, *Chem. Asian J.* **2015**, *10*, 563–567.
[32] B. Lkhagvadulam, J. H. Kim, I. Yoon, Y. K. Shim, *J. Porphyrins Phthalocyanines* **2012**, *16*, 331–340.
[33] B. Lkhagvadulam, J. H. Kim, I. Yoon, Y. K. Shim, *BioMed Res. Int.* **2013**, *V2013*, Article ID 720579, 10 pages.
[34] J.-G. Kwon, I.-S. Song, M.-S. Kim, B. H. Lee, J. H. Kim, I. Yoon, Y. K. Shim, N. Kim, J. Han, J. B. Youm, *Integr. Med. Res.* **2013**, *2*, 106–111.
[35] D. Demberelnyamba, M. Ariunaa, Y. K. Shim, *Int. J. Mol. Sci.* **2008**, *9*, 864–871.
[36] I. Yoon, J. H. Kim, J. Z. Li, W. K. Lee, Y. K. Shim, *Inorg. Chem.* **2014**, *53*, 3–5.

[37] M. V. Vasylyev, R. Neumann, *J. Am. Chem. Soc.* **2004**, *126*, 884–890.
[38] G.-G. Gao, L. Xu, W.-J. Wang, X.-S. Qu, H. Liu, Y.-Y. Yang, *Inorg. Chem.* **2008**, *47*, 2325–2333.
[39] H. Yanagie, A. Ogata, S. Mitsui, T. Hisa, T. Yamase, M. Eriguchi, *Biomed. Pharmacother.* **2006**, *60*, 349–352.
[40] H. Thomadaki, A. Karaliota, C. Litos, A. Scorilas, *J. Med. Chem.* **2007**, *50*, 1316–1321.
[41] R. Guo, Y. Cheng, D. Ding, X. Li, L. Zhang, X. Jiang, B. Liu, *Macromol. Biosci.* **2011**, *11*, 839–847.
[42] X. Wei, K. Ma, Y. Cheng, L. Sun, D. Chen, X. Zhao, H. Lu, B. Song, K. Yang, P. Jia, *ACS Appl. Polym. Mater.* **2020**, *2*, 2541–2549.
[43] Y. Fang, T. Liu, C. Xing, J. Chang, M. Li, *Int. J. Pharm.* **2020**, *591*, 119990.
[44] Azizullah, A. Haider, U. Kortz, S. A. Joshi, J. Iqbal, *ChemistrySelect* **2017**, *2*, 5905–5912.
[45] E. S. Kang, T. H. Lee, Y. Liu, K.-H. Han, W. K. Lee, I. Yoon, *Int. J. Mol. Sci.* **2019**, *20*, 4344.
[46] J.-E. Chang, Y. Liu, T. H. Lee, W. K. Lee, I. Yoon, K. Kim, *Int. J. Mol. Sci.* **2018**, *19*, 1596.
[47] I. Yoon, H. S. Park, B. C. Cui, J. H. Kim, Y. K. Shim, *Bull. Korean Chem. Soc.* **2011**, *32*, 169–174.
[48] B. C. Cui, I. Yoon, J. Z. Li, Y. K. Shim, *J. Chem. Pharm.* **2013**, *5*, 818–823.
[49] Y. Yang, J. He, X. Wang, B. Li, J. Liu, *Transit. Met. Chem.* **2004**, *29*, 96–99.
[50] Y. Liu, M. S. Lee, S. H. Lee, H. H. Song, B. S. Baek, W. K. Lee, Y.-J. Kim, I. Yoon, *ChemNanoMat* **2021**, *7*, 165–173.
[51] Y. Liu, T. H. Lee, S. H. Lee, J. Li, W. K. Lee, I. Yoon, *ChemNanoMat* **2020**, *6*, 610–617.
[52] B. Jana, A. P. Thomas, S. Kim, I. S. Lee, H. Choi, S. Jin, S. A. Park, S. K. Min, C. Kim, J.-H. Ryu, *Chem. Eur. J.* **2020**, *26*, 10695–10701.
[53] Y. Liu, Z. Zhou, X. Lin, X. Xiong, R. Zhou, M. Zhou, Y. Huang, *Biomacromolecules* **2019**, *20*, 3755–3766.
[54] D. Zhang, L. Wen, R. Huang, H. Wang, X. Hu, D. Xing, *Biomaterials* **2018**, *153*, 14–26.
[55] K. M. Smith, D. A. Goff, D. J. Simpson, *J. Am. Chem. Soc.* **1985**, *107*, 4946–4954.
[56] C. Sanchez, J. Livage, J. P. Launay, M. Fournier, Y. Jeannin, *J. Am. Chem. Soc.* **1982**, *104*, 3194–3202.
[57] G. Zheng, A. Graham, M. Shibata, J. R. Missert, A. R. Oseroff, T. J. Dougherty, R. K. Pandey, *J. Org. Chem.* **2001**, *66*, 8709–8716.
[58] X. Liang, X. Li, X. Yue, Z. Dai, *Angew. Chem. Int. Ed.* **2011**, *50*, 11622–11627; *Angew. Chem.* **2011**, *123*, 11826–11831.
[59] W.-S. Kuo, C.-N. Chang, Y.-T. Chang, M.-H. Yang, Y.-H. Chien, S.-J. Chen, C.-S. Yeh, *Angew. Chem. Int. Ed.* **2010**, *49*, 2711–2715; *Angew. Chem.* **2010**, *122*, 2771–2775.
[60] I. Yoon, H. S. Park, B. C. Cui, J. Z. Li, J. H. Kim, B. Lkhagvadulam, Y. K. Shim, *Bull. Korean Chem. Soc.* **2011**, *32*, 2981–2987.
[61] Cationic PS for dark toxicity, high cellular uptake corresponding to the electrostatic interaction of the positively charged PS surface and the negatively charged plasma membrane of mammalian cells, see: G.-D. Zhang, A. Harada, N. Nishiyama, D.-L. Jiang, H. Koyama, T. Aida, K. Kataoka, *J. Controlled Release* **2003**, *93*, 141–150.
[62] F. Ricchelli, L. Franchi, G. Miotto, L. Borsetto, S. Gobbo, P. Nikolov, J. C. Bommer, E. Reddi, *Int. J. Biochem. Cell Biol.* **2005**, *37*, 306–319.
[63] K. Wang, C. T. Poon, C. Y. Choi, W.-K. Wong, D. W. J. Kwong, F. Q. Yu, H. Zhang, Z. Y. Li, *J. Porphyrins Phthalocyanines* **2012**, *16*, 85–92.
[64] B. Kofler, A. Romani, C. Pritz, T. B. Steinbichler, V. H. Schartinger, H. Riechelmann, J. Dudas, *Int. J. Mol. Sci.* **2018**, *19*, 1107.
[65] L. Zhang, J. P. Lei, F. J. Ma, P. H. Ling, J. T. Liu, H. X. Ju, *Chem. Commun.* **2015**, *51*, 10831–10834.
[66] T. Yue, X. Zhang, *ACS Nano* **2012**, *6*, 3196–3205.
[67] G. Zheng, W. R. Potter, S. H. Camacho, J. R. Missert, G. Wang, D. A. Bellnier, B. W. Henderson, M. A. J. Rodgers, T. J. Dougherty, R. K. Pandey, *J. Med. Chem.* **2001**, *44*, 1540–1559.
[68] In this paper, we used different method to synthesize **2** compared with previous report (Ref. 19) by us. All of the characterization data were identical with the report.
[69] J. Z. Li, Synthesis and Properties of New Chlorophyll Derivatives Conjugated with Trolox, Cationic Moieties or Hydrazones for Application in Photodynamic Therapy. Ph.D. Dissertation, University of Inje, 2012.

Manuscript received: June 4, 2021
Revised manuscript received: July 6, 2021
Accepted manuscript online: July 11, 2021

FULL PAPERS

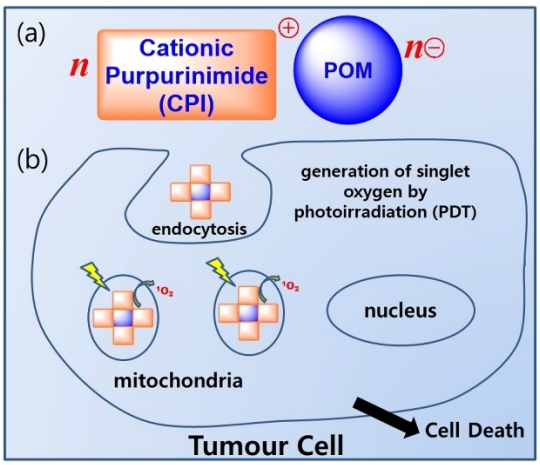

T. H. Lee, Dr. Y. Liu, H. J. Kim, S. H. Lee, H. H. Song, Prof. Dr. Y. K. Shim, Prof. Dr. W. K. Lee, Prof. Dr. I. Yoon**

CPI–POM supramolecular complexes, resulting from the electrostatic interactions between CPI and polyanionic POM, those exhibited high cellular uptake followed by mitochondrial targeting of CPI–POM complexes into tumour cells through endocytosis, causing cell death after photogeneration of $^1O_2$, resulting in enhanced photodynamic activity with reduced dark toxicity.